Research Article

A New Method of Synthesizing Black Birnessite Nanoparticles: From Brown to Black Birnessite with Nanostructures

Marcos A. Cheney,[1] Pradip K. Bhowmik,[2] Shizhi Qian,[3] Sang W. Joo,[4] Wensheng Hou,[5] and Joseph M. Okoh[1]

[1] *Department of Natural Sciences, University of Maryland Eastern Shore, Princess Anne, MD 21853, USA*

[2] *Department of Chemistry, University of Nevada Las Vegas, 4505 Maryland Parkway, Las Vegas, NV 89154, USA*

[3] *Department of Aerospace Engineering, Old Dominion University, Norfolk, VA 23529, USA*

[4] *School of Mechanical Engineering, Yeungnam University, Gyongsan 712-749, South Korea*

[5] *Department of Biomedical Engineering, Chongqing University, Chongqing 400044, China*

Correspondence should be addressed to Shizhi Qian, sqian@odu.edu

A new method for preparing black birnessite nanoparticles is introduced. The initial synthesis process resembles the classical McKenzie method of preparing brown birnessite except for slower cooling and closing the system from the ambient air. Subsequent process, including wet-aging at 7°C for 48 hours, overnight freezing, and lyophilization, is shown to convert the brown birnessite into black birnessite with complex nanomorphology with folded sheets and spirals. Characterization of the product is performed by X-ray diffraction (XRD), transmission electron microscopy (TEM), high-resolution transmission electron microscopy (HRTEM), thermogravimetric analysis (TGA), and N_2 adsorption (BET) techniques. Wet-aging and lyophilization times are shown to affect the architecture of the product. XRD patterns show a single phase corresponding to a semicrystalline birnessite-based manganese oxide. TEM studies suggest its fibrous and petal-like structures. The HRTEM images at 5 and 10 nm length scales reveal the fibrils in folding sheets and also show filamentary breaks. The BET surface area of this nanomaterial was found to be $10.6\,m^2/g$. The TGA measurement demonstrated that it possessed an excellent thermal stability up to 400°C. Layer-structured black birnessite nanomaterial containing sheets, spirals, and filamentary breaks can be produced at low temperature ($-49°C$) from brown birnessite without the use of cross-linking reagents.

1. INTRODUCTION

There is an increasing interest in layer-structured materials due to their vast areas of applications, such as catalysis, ion-sieves, and rechargeable batteries [1–3]. Birnessite-type manganese oxide, MnO_2, is a layer-structured mineral containing edge-shared MnO_6 octahedral with a d-spacing of ca. 7 Å, which renders mobility of interlayer cations without a structural change [4]. Birnessite nanoparticles thus have many potential applications, and the method for preparing them with desired micro- and nanostructure has been a subject of intensive study.

A number of synthetic processes for preparing layer-structured brown birnessite with microscale structures have existed since the early report of McKenzie [5], including oxidation of Mn(II) in basic solution [6], redox reaction between Mn(II) and MnO_4^- [7], reduction of MnO_4^- using

different routes such as sol gel [8], reaction of HCl with MnO_4^- followed by cationic exchange, and by oxidation of Mn(II) using O_2, $K_2S_2O_8$, and H_2O_2. Synthesis methods for preparing black birnessite with nanostructures are relatively scarce, although preparation of nanocrystalline MnO_2 has been attracting special interest [9]. One dimensional (1D) single-crystal nanowires of α-MnO_2 and β-MnO_2 have been synthesized via hydrothermal route using $MnSO_4$ and oxidizing agents, such as $(NH_4)_2S_2O_8$ or $KMnO_4$ [10]. Nanowires of α-MnO_2 are also synthesized using coordination polymers [11–13]. Birnessite nanoparticles with hexagonal layer structure with dendritic morphology are synthesized based on the reduction of $KMnO_4$ in dilute aqueous H_2SO_4 with initial stirring, followed by wet-aging time and air drying [14]. More recently, birnessite has also been prepared by the electrochemical stimulation of Mn_3O_4 in Na_2SO_4 solution to be used as electrochemical

supercapacitors [15, 16] and semiconductors [17]. Pillared birnessite nanosheets have been prepared by an ion-exchange method [18]. Transition metal-doped birnessite has also been prepared from surfactant-free nonaqueous sol gel routes [19]. Nevertheless, birnessite structural details, crystal chemistry, and morphological prediction remain elusive. Birnessite-type manganese oxides are a two-dimensional (2D) layer-structure material and an important precursor for the synthesis of tunnel-structure manganese oxides [20]. It forms by a regular distribution of Mn vacancies in the MnO crystal matrix. The structure is generated by the removal of Mn atoms from the corners and faces in a doubled unit cell of MnO [19].

Some of the aforementioned methods generate birnessite nanofibers with interesting and desirable nanostructures. Synthesis of black birnessite nanoparticles of inorganic clusters with complex architecture, such as sheets, spiral, and petal-like morphology, however, is more difficult. Here, we report the synthesis of such particles from the conversion of brown birnessite (same batch) without the use of chiral solvents, templates, or cross-linking reagents. The classical synthesis process of McKenzie [5] is chosen with minor modifications to produce intermediate brown birnessite, which is then converted to more crystalline black birnessite via a postprocess of slow cooling, cold wet-aging, freezing, and lyophilization.

The purpose of the current report is straightforward. As we report a new synthesis method for black birnessite nanoparticles with an intriguing morphology, we show that complex nanostructures can be created by purely physical treatments added to otherwise brown-birnessite preparing processes. Cheney et al. [14] have shown that a synthesis method for brown birnessite turns into that for black birnessite with dendritic nanostructure by a simple preprocess of 10-minute stirring. In this study, we show the same by a simple postprocess.

2. EXPERIMENT

2.1. Synthesis

The synthesis can be divided into two steps: production of the intermediate brown birnessite and conversion into black birnessite. The first step is composed of a slow dropwise (86 drops/min) addition of 0.5 L of 2 M hydrochloric acid (HCl), with a vigorous stirring at 300 rpm, into a 4 L beaker containing a solution, prepared by dissolving 1.0 mol of $KMnO_4$ (158 g) in a 2.5 L of 18 MΩ water, and then heating at 95°C. Here, the beaker is covered with a large watch glass with a thermometer inserted through a protuberance of 1 inch in diameter. Through the protuberance, HCl is added dropwise over a period of 2 hours using a separatory funnel after which the thermometer is removed. The beaker is then completely covered with the watch glass, boiled for 10 minutes, and then wrapped with an aluminum foil to prevent rapid cooling. The reaction produces chlorine gas, which keeps air from entering the beaker during the process. The reaction is completed in 2 hours, producing brown manganese oxide. After the stirring was stopped, particles

began to settle under a cloud of chlorine gas. The coloration of the supernatant solution can be detected visually.

The second step of conversion to black birnessite starts with a slow cooling of the beaker to room temperature. The mixture is left in the hood overnight. Subsequently, the mixture is wet-aged for 48 hours at 7°C. The brown slurry formed is then centrifuged at 2800 rpm, decanted, washed 13 times with 18 MΩ water, and placed in a standard freezer overnight. The samples are then freeze-dried (lyophilized) at 0.7 mbar pressure and −49°C for 3 days, after which they turned black.

2.2. Characterization

The manganese oxides are characterized by X-ray powder diffraction (XRD) using a PANalytical X'Pert PRO X-ray diffractometer with a Cu K_α radiation (40 KV, 40 mA), and an X'Celerator solid state detector. The samples are prepared by suspending the oxide and the SRM in ethanol to form a slurry. The oxide powders are prepared on a low-background silicon sample holder with the addition of an internal standard (NIST SRM 640c, $a = 5.43088$ Å). The patterns are recorded at room temperature with step sizes of 0.008°, 2θ, and 50 seconds. The phase constitutions are characterized using the International Center for Diffraction Data (ICDD) base for powder diffraction data. Crystallography of the phase constitution is confirmed using Rietveld refinement (Topas 2.1 Bruker AXS) and the International Crystal Structure Data (ICSD) base.

The specific surface areas of the synthesized oxides are measured at 77°K using a Gemini 2370 (Micromeritics, GA, USA) surface and porosimetry instrument. The surface area is calculated from the Brunauer-Emmett-Teller (BET) analysis of N_2 adsorption isotherm obtained after degassing and drying the sample at 200°C for 24 hours [21].

Transmission electron microscopy (TEM) images are obtained using a Tecnai G^2 F30 S-Twin TEM instrument. The TEM operates at 300 KV using a field emission gun in Schottky mode as an electron source. The samples for TEM analysis are prepared by placing 3 mg of the freeze-dried solid manganese oxide in 10 mL of 2-propanol, and sonication for 5 minutes for homogeneity. One drop of the slurry is deposited on a holey carbon-coated copper grid for analysis.

The thermogravimetric (TGA) measurements are performed with a TA 2100 instrument in the range of 0 to 600°C at a heating rate of 20°C/min under nitrogen.
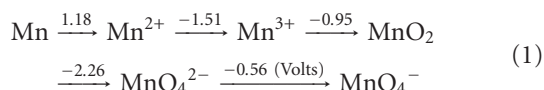
3. RESULTS AND DISCUSSION

3.1. Creation of inorganic nanosized sheets and spiral clusters with complex architecture

The synthesis method of McKenzie that produces microscale brown particles resembles the first step of producing intermediate brown birnessite in the new method described above. In the McKenzie method, 2 M of HCl is added more rapidly at 200 drops/min to 1 M of $KMnO_4$, and the container is open to the air with a less vigorous stirring of 150 rpm at 95°C. The solution is then cooled rapidly
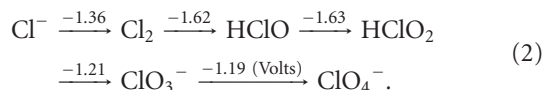
to room temperature with no aging time, and immediately centrifuged, washed, and lyophilized. The room temperature and 7°C wet-aging and overnight freezing are missing, which results in brown birnessite with drastically different morphology. The missing processes thus are responsible for the curved nanosheets with petal-like morphology and clover-like nanoclusters of layer structure exhibited in the black birnessite produced with the new method.

The synthesis consists of the reduction of permanganate ions by concentrated hydrochloric acid (HCl) in acidic conditions in a closed system and with aging time. In this reaction, permanganate is reduced to the lower valence Mn(IV) species in acidic conditionsvia an intermediate state Mn(III) [22] according to the following redox potential diagrams [23]:
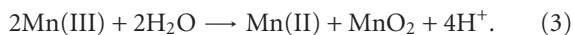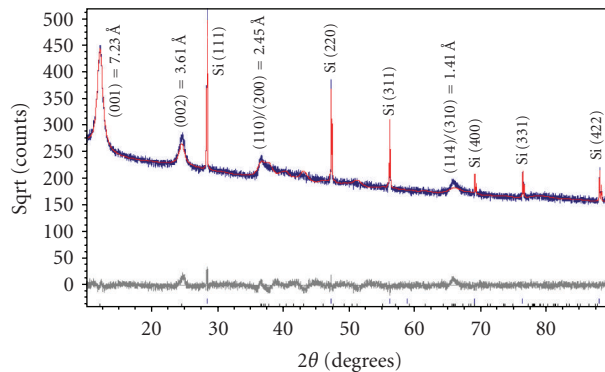
manganese

$$Mn \xrightarrow{1.18} Mn^{2+} \xrightarrow{-1.51} Mn^{3+} \xrightarrow{-0.95} MnO_2 \tag{1}$$
$$\xrightarrow{-2.26} MnO_4{}^{2-} \xrightarrow{-0.56 \text{ (Volts)}} MnO_4{}^{-}$$

chloride

$$Cl^{-} \xrightarrow{-1.36} Cl_2 \xrightarrow{-1.62} HClO \xrightarrow{-1.63} HClO_2 \tag{2}$$
$$\xrightarrow{-1.21} ClO_3{}^{-} \xrightarrow{-1.19 \text{ (Volts)}} ClO_4{}^{-}.$$

The reduction potentials suggest that the manganic ion, Mn(III), produced by the reduction of permanganate ion by HCl, is unstable in respect to the following decomposition [23]:

$$2Mn(III) + 2H_2O \longrightarrow Mn(II) + MnO_2 + 4H^+. \tag{3}$$

The Mn(II) produced is then oxidized to Mn(IV) by permanganate or MnO_2. This may be a reason why the XRD and XANES analyses (not shown) showed no Mn(III) present in the sample. This result is rather remarkable because nonbiogenic and biogenic manganese oxides are known to exhibit Mn in the +3 oxidation state probably due to (3) [24]. The production of K-birnessite or H-birnessite containing only Mn(IV), via a chemical protocol, is indeed more challenging. In biogenic manganese oxides, Mn(III) may be stabilized by organic complexing agents found in cell material. In the new synthesis method developed, it appears that the Cl^- ion does not have a significant effect on stabilizing Mn(III), which otherwise would have been detected as a different phase in the XRD. This is in spite of the high concentration of Cl^- present in the system. Also, in our method, the reaction between HCl and $MnO_4{}^-$ does not seem to be complete, as evidenced by the persistent color of the solution at the end of the synthesis. This observation is surprising because the concentration of HCl is twice the concentration of $MnO_4{}^-$ and, according to the redox potentials shown in (1) and (2) above, this reaction is likely to be complete. Therefore, another phenomenon may be involved in the inhibition of this reaction, and influences the amount of nanomaterial formed. We speculate that the cloud of chlorine gas formed as a byproduct, which is accumulated in the headspace of the closed container, might

(a)
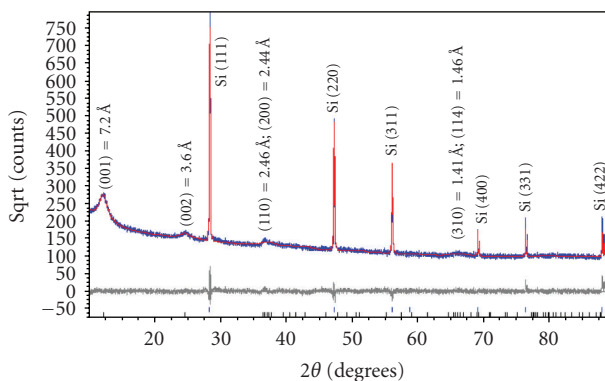
(b)

Figure 1: X-ray powder diffraction of the synthesized manganese oxide. (a) Black birnessite produced by our method, and (b) brown birnessite produced by the McKenzie method.

have influenced the reaction by limiting the presence of oxygen. The brown-colored solid produced then is converted to black solid through overnight freezing and subsequent lyophilization process at 0.7 mbar pressure and −49°C for 3 days. This result is surprising because all methods of synthesis of, or conversion to, black birnessites reported to date are carried out at high (95°C) temperatures [24–28].

3.2. X-ray powder diffraction

The phases formed by the new method described above are characterized by XRD in comparisonwith those prepared by the McKenzie method [5]. Figure 1(a) shows the XRDpatterns of nanosized semicrystalline black birnessite obtained by the new method, along with the analysis ofthe data using the Rietveld refinement. The XRD pattern of brown birnessite obtained using the McKenzie method withno aging time is shown in Figure 1(b). Although these graphs indicate that the profile parameter of the diffraction peaks of black and brown birnessite are similar, it is seen that the crystallinity is increased with the aging time and the diffraction peaks of black birnessite have become more defined.

The XRD patterns of the black birnessite shown in Figure 1(a) suggest that cold aging process and lyophilization
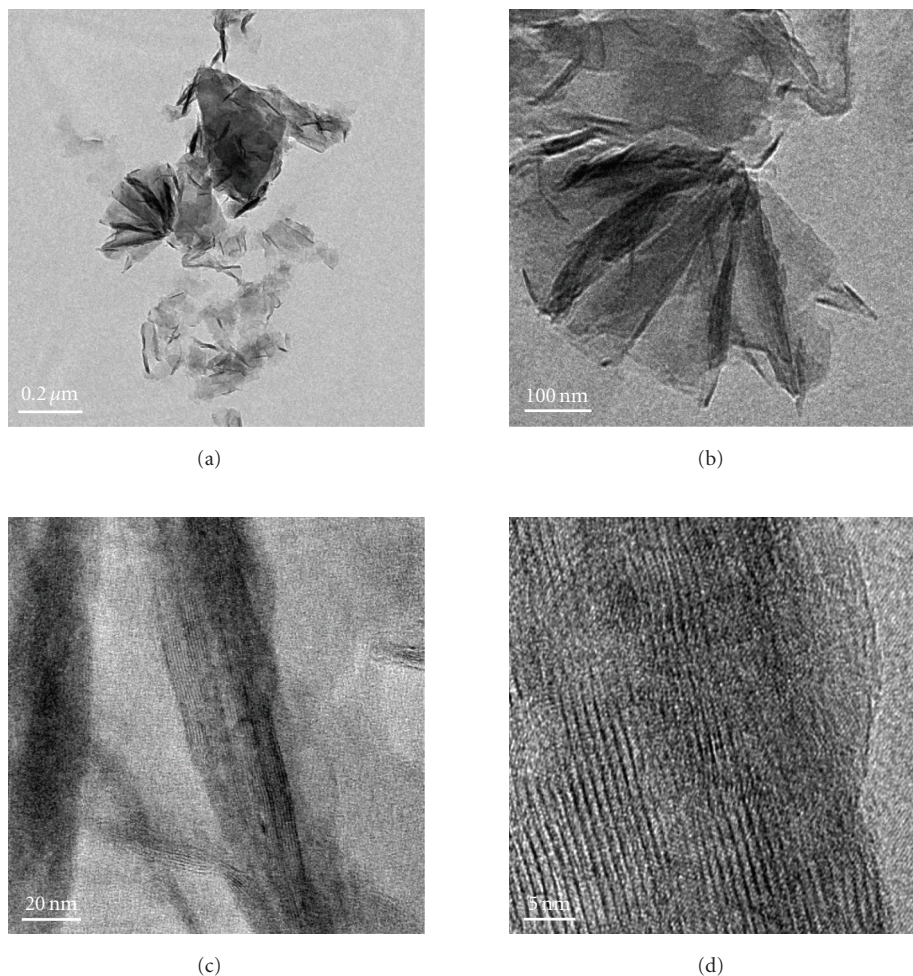
(a)

(b)

(c)

(d)

FIGURE 2: Transmission electron microscopy (a) and (b) and high-resolution transmission electron microscopy (c) and (d) images of the black birnessite nanomaterial synthesized by our method.

affect the crystallinity of final product. Based on XRD and Rietveld analysis, we can refine the lattice parameter of birnessite to a = 4.944(3) Å, b = 2.834(2) Å, c = 7.295(1) Å, β = 97.8(1) Å, and the space group $C2/m$ is confirmed. Relative peak intensities of (001), (002), (200)/(110), and (114)/(310) are calculated to a refinement residual (R_{wp}) of 4%. The calculated XRD pattern further reveals the semicrystalline character of the specimen and lattice planes of minor intensities that are not developed. The layered structure of birnessite has a repeat distance of 7.23 Å corresponding to (001) lattice plane of black birnessite, as for the K-rich [29] or the H-birnessite [24]. The peak profiles indicate crystal sizes in the range of 14-15 nm, which is also confirmed by HRTEM. In the case of the McKenzie method (open system and no aging time), the above reaction produced specimens of lower crystallinity, as indicated by the relative peak intensities and the peak profiles using Rietveld analysis (Figure 1(b)). The XRD pattern also shows a single phase with the strongest d-spacing (001) of 7.2 Å, corresponding to brown birnessite. This reaction is very sensitive to experimental conditions used. Minor modification of the original procedure, that is, slow addition

of HCl and with no cold aging time, results in the formation of nanosized crystals mixed with large crystals [29, 30]. This may be due to a rapid and unrestricted reaction between Mn(III) and Mn(IV), which are formed by the oxidation of Mn(II) by permanganate at low pH. The oxidation of Mn(II) by MnO_4^- is reported to be autocatalytic [16], and can be influenced by the increased concentration of Mn(II) in solution from (3). The repeated distances (d-spacing) of 7.23 Å and 7.20 Å for both black and brown birnessites suggest that there is at least one water layer present in the oxides with the former being a little more hygroscopic.

3.3. TEM and HRTEM studies

The nanostructures of both black and brown birnessites are studied using TEM. Figure 2 shows the TEM images and petal-like distribution obtained for nanosized black birnessite. The sheets and petal-like architecture are shown in Figures 2(a) and 2(b). High-resolution transmission electron microscopy (HRTEM) images, shown in Figures 2(c) and 2(d), display the crystal structure of the fibrils (010) direction. Figure 2(c) shows the edge of a sheet suggesting

that the sheets fold in a dough-like manner, producing a plant stem-like appearance. This micrograph also shows a defect in the arrangement as petiole (protuberance) from the stem. The high-resolution image in Figure 2(d) shows lattice fringes of the fibrils with a translation of 7-8 Å which correspond well with (001) lattice plane determined by XRD.

The manganese oxides synthesized by the new method show a petal-like and fibrous morphology of birnessite-type materials (Figures 2(a)–2(c)). The TEM reveals that the length of the clusters appears to be in the 300 nm range and the width in the order of 200 nm, suggesting nanosized clusters. The TEM also shows that curled architectures are produced at the top of the petals. Formation of these clusters appears to depend on the cold-aging time and the temperature of lyophilization.

Figure 3 shows the TEM images and fiber distribution obtained for brown birnessite. The fiber architecture is represented in Figures 3(a) and 3(b). Nanosized clusters can be observed with some twisting in a coil-like manner. The HRTEM images shown in Figures 3(c) and 3(d) also suggest an orientation of some of the fibers in (010) direction. However, the dominant lattice fringes in the high-resolution images as shown indicate a repetition of the (001) lattice plane (Figures 3(e) and 3(f)).

In the case of brown birnessite nanoclusters, the TEM images show a dendritic morphology in the 100 nm range, as shown in Figures 3(a) and 3(b), which can be compared with echinate spines similar to the dandelion pollen grains, made from other inorganic materials reported by Hall et al. [30]. However, in this material, the dendrites are covered with a veil which can partly be seen in the circled region in Figure 3(d) as single sheet. At 20 nm length scale, sheets and coil-like morphologies are also detected, and the veil, seen at 100 nm, becomes more apparent, suggesting that it is composed of a small single sheet. It is interesting to learn that the dendritic appearance observed in this image is actually caused by the folding of small sheets. Figures 3(a), 3(b), and 1 also suggest that the nanoclusters of the birnessite appear crystalline and link together to form larger clusters with no apparent crystallographic orientation. To accurately characterize birnessite-type material, a combination of complementary analytical tools like HRTEM and XRD are essential.

HRTEM studies show that most of the black birnessite nanofibers are oriented in the (010) direction (zone-axis direction), and the lattice fringes reflecting the (001) lattice plane become visible in Figures 2(c) and 2(d). At 1 000 000-fold magnification, the veins along the radial direction of the fiber are clearly seen, indicative of layered structure (Figure 2(d)). Additionally, some imperfections in the arrangement of the fibers can also be seen in Figure 2(c). These imperfections suggest that the sheets fold in a dough-like manner, producing stem-like appearance of a plant. Furthermore, this micrograph also shows a growth in the arrangement as petiole (protuberance) from the stem. This result supports the observation that the formation of the petal-like sheets may be due to the growth of a cluster of fibrous units along the c- axis and we speculate that the high amount of structure defects of the semicrystalline material

produce peak broadening in the XRD. The development of a petiole is intriguing given the fact that this kind of growth is seen only in living organisms such as plants but not in inorganic materials made without templates. This work shows that the production of the nanoscale fibers seems to be a key step for the formation of petal-like morphology. The detailed mechanism for the formation of these interesting shapes at low pH is not presently known. However, we speculate that the formation of the sheets may be due to a structural control of crystal growth guided by osmotic pressure [31] and the unreacted Cl^- ion. The sheets and petal-like architecture thus can be produced by a growth of the corn rows on the surface of clusters made of fibrils. The path then would be a branching direction (horizontal) followed by a growth direction (vertical) of the subunits. The stacking of the subunits in the vertical direction reaches a point that the units begin to fold forming the petal-like architecture. It is known that fibers or rods attract each other along their elongated sides forming clusters [28]. This phenomenon is evident in the TEM images in Figures 2(a)–2(c). What is intriguing is that the petal-like architecture observed in these inorganic nanomaterials is indeed similar to the structures observed in biogenic manganese oxides [24] and in self-assembled organic systems [32]. We support the view of Terada et al. [33] that the phenomenon that gives rise to the observed coil and curved architectures in both inorganic and biological materials may be related to the flexibility in the development processes of these morphologies. A distortion in the development of the subunits promotes curved sheets that tend to decrease their surface area when rolled up. This may be one explanation as to why the surface area of black birnessite ($10.6 \, m^2g^{-1}$), which contains larger sheets, is lower than that of the brown birnessite ($36.2 \, m^2g^{-1}$), which contains much smaller sheets of dendritic morphology. The brown birnessite produced by the McKenzie method consists of small clusters linked together to form larger particles of micron size. The method reported here is highly reproducible if the synthetic parameters such as temperature, stirring rate, and the speed of the addition of one reactant into another are rigorously controlled.

3.4. Thermal stability of the birnessite nanofibers

The TGA measurements of the synthesized materials using the new method and the McKenzie method are shown in Figure 4. The TGA profiles for both samples look similar and show that there are two weight losses in both samples; the first consisting of about 10% in the range of 147–160°C and the second consisting of about 13% for the McKenzie method and about 14% for the sample prepared using the new method in the temperature range of 400–446°C. There is a slight gain in mass observed in the range of 440–475°C. The thermal stability of the samples seems unaffected by the wet-aging process.

The first weight loss of 10% indicated by the thermogram is due to loss of loosely bound water indicating the samples are hygroscopic. The second loss of 13% in the temperature range of 422 to 443°C is attributed to chemically bound water and oxygen from the oxide [32]. The weight loss of the
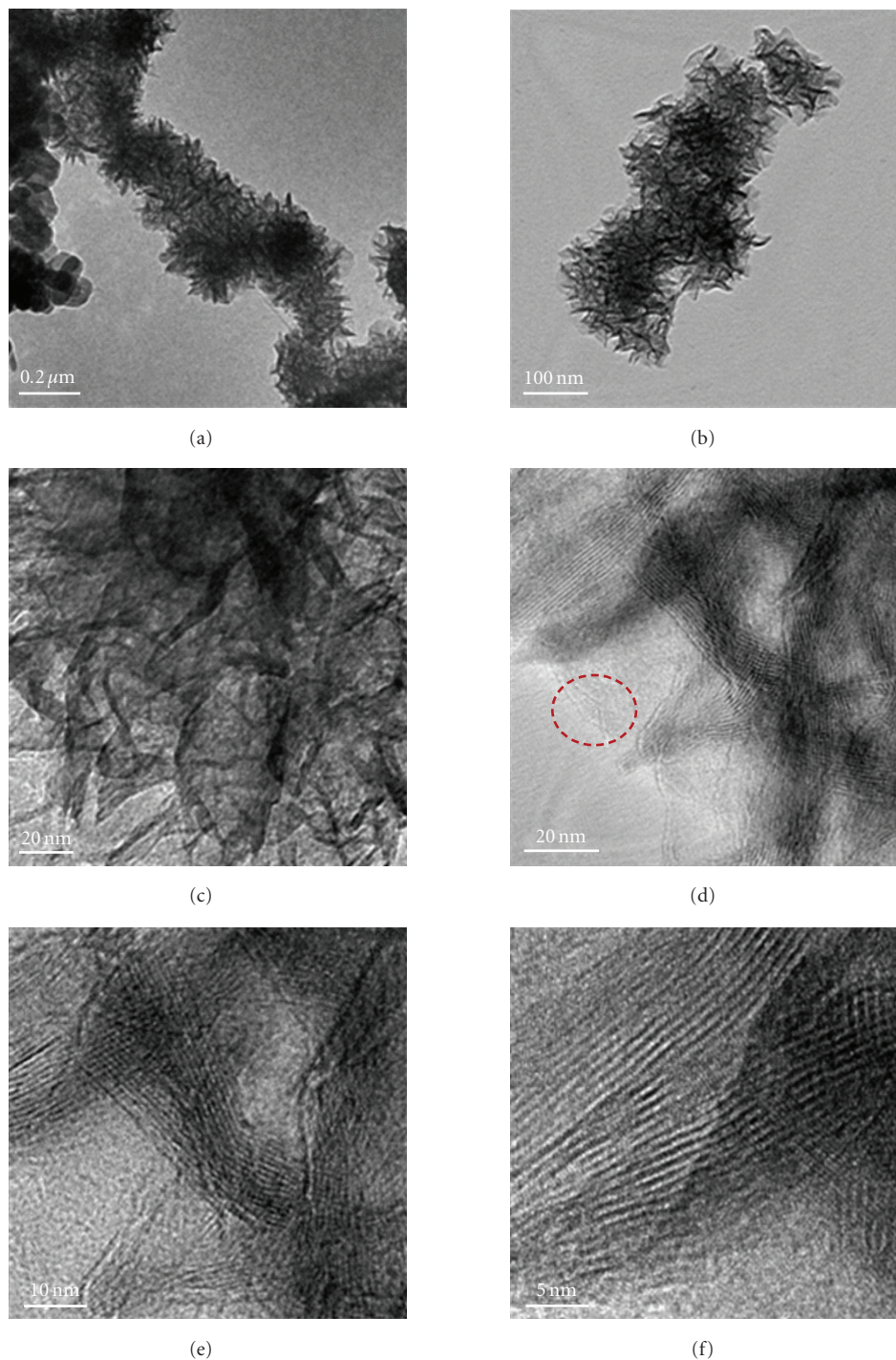
(a)

(b)

(c)

(d)

(e)

(f)

FIGURE 3: Transmission electron microscopy (a) and (b) and high-resolution transmission electron microscopy (c)–(f) images of the brown birnessite produced by the McKenzie method.

black birnessite in this temperaturerange is slightly higher than the brown birnessite, suggesting that this material is morehygroscopic and correlates well with a d-spacing of 7.22 Å observed in the XRD. The weight gained in the temperature range of 443–463°C can be attributed to migration of the Mn_{layer} to the new vacant sites produced by the partial reduction of Mn^{4+} to Mn^{3+} and subsequent oxidation of Mn^{3+} [32].

3.5. Surface area

The surface areas estimated for the black and brown birnessites prepared by the new and the McKenzie method, respectively, are listed in Table 1. The surface areaof the black nanobirnessite-type manganeseoxide turns out to be lower (10.6 m²/g) than that produced by using the McKenzie method. The aging time seems to affect the surface area.
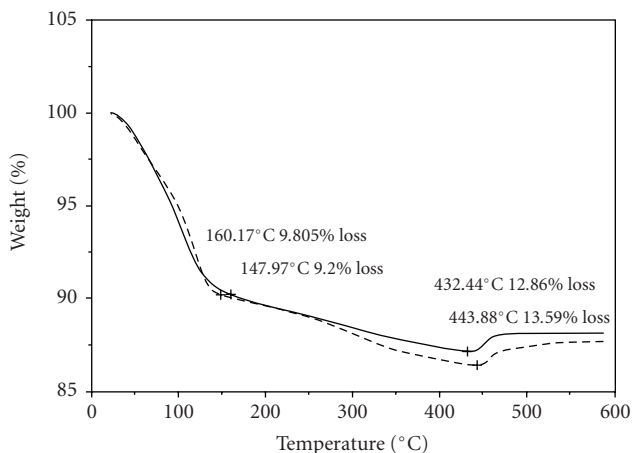
FIGURE 4: Thermogravimetric analysis (TGA) of the synthetic manganese oxides. Black birnessite nanomaterial produced by our method (dashed line), and brown birnessite produced by the McKenzie method (solid line).

TABLE 1: Surface areas of standard material (Kaolinite) and synthesized nanosized black and brown birnessites.

Sample	Surface area m^{2}g^{-1}
Kaolinite—SRM lot # 19672-18	14.9($\pm$1)
K-MnO$_2$ (black birnessite synthesized by the developed method)	10.6($\pm$1)
K-MnO$_2$ (brown birnessite synthesized by the McKenzie method)	36.2($\pm$1)

4. CONCLUDING REMARKS

In spite of all the research reported in the literature and in progress, birnessite structural details, crystal chemistry, and morphological prediction remain elusive. This is due, in part, to a lack of valid concepts and principles necessary for reproducible size, surface area, and morphology between synthetic batches.

In this spirit, a new synthesis method for black birnessite nanoparticles is introduced. The method first produces intermediate brown birnessite via the classical McKenzie method for preparing brown birnessite with minor modifications. The conversion of the brown to black birnessite is accomplished by purely physical treatments of wet-aging, freezing, and lyophilization. This new synthesis method is notable at least for the following two reasons. First, the method generates novel nanostructures with sheets, spiral, and petal-like morphology. Secondly, while all synthesis or conversion methods for black birnessite apply heating, the black birnessite here is prepared by cooling and freezing.

ACKNOWLEDGMENTS

REFERENCES

[1] A. R. Armstrong and P. G. Bruce, "Synthesis of layered LiMnO$_2$ as an electrode for rechargeable lithium batteries," *Nature*, vol. 381, no. 6582, pp. 499–500, 1996.

[2] S. L. Brock, N. Duan, Z. R. Tian, O. Giraldo, H. Zhou, and S. L. Suib, "A review of porous manganese oxide materials," *Chemistry of Materials*, vol. 10, no. 10, pp. 2619–2628, 1998.

[3] Q. Feng, H. Kanoh, and K. Ooi, "Manganese oxide porous crystals," *Journal of Materials Chemistry*, vol. 9, no. 2, pp. 319–333, 1999.

[4] R. Ma, Y. Bando, L. Zhang, and T. Sasaki, "Layered MnO$_2$ nanobelts: hydrothermal synthesis and electrochemical measurements," *Advanced Materials*, vol. 16, no. 11, pp. 918–922, 2004.

[5] R. M. McKenzie, "Synthesis of birnessite, cryptomelane, and some other oxides and hydroxides of manganese," *Mineralogical Magazine*, vol. 38, pp. 493–502, 1971.

[6] D. C. Golden, C. C. Chen, and J. B. Dixon, "Synthesis of todorokite," *Science*, vol. 231, no. 4739, pp. 717–719, 1986.

[7] J. Luo and S. L. Suib, "Formation and transformation of mesoporous and layered manganese oxides in the presence of long-chain ammonium hydroxides," *Chemical Communications*, no. 11, pp. 1031–1032, 1997.

[8] J. Cai, J. Liu, and S. L. Suib, "Preparative parameters and framework dopant effects in the synthesis of layer-structure birnessite by air oxidation," *Chemistry of Materials*, vol. 14, no. 5, pp. 2071–2077, 2002.

[9] M. Tsuji, S. Komarneni, Y. Tamaura, and M. Abe, "Cation exchange properties of a layered manganic acid," *Materials Research Bulletin*, vol. 27, no. 6, pp. 741–751, 1992.

[10] J. Luo, Q. Zhang, A. Huang, and S. L. Suib, "Total oxidation of volatile organic compounds with hydrophobic cryptomelane-type octahedral molecular sieves," *Microporous and Mesoporous Materials*, vol. 35-36, pp. 209–217, 2000.

[11] T. D. Xiao, P. R. Strutt, M. Benaissa, H. Chen, and B. H. Kear, "Synthesis of high active-site density nanofibrous MnO$_2$-base materials with enhanced permeabilities," *Nanostructured Materials*, vol. 10, no. 6, pp. 1051–1061, 1998.

[12] Y. Xiong, Y. Xie, Z. Li, and C. Wu, "Growth of well-aligned γ-MnO$_2$ monocrystalline nanowires through a coordination-polymer-precursor route," *Chemistry: A European Journal*, vol. 9, no. 7, pp. 1645–1651, 2003.

[13] X. Wang and Y. Li, "Selected-control hydrothermal synthesis of α- and β-MnO$_2$ single crystal nanowires," *Journal of the American Chemical Society*, vol. 124, no. 12, pp. 2880–2881, 2002.

[14] M. A. Cheney, P. K. Bhowmik, S. Moriuchi, M. Villalobos, S. Qian, and S. W. Joo, "The effect of stirring on the morphology of birnessite nanoparticles," *Journal of Nanomaterials*, vol. 2008, Article ID 168716, 9 pages, 2008.

[15] S. Komaba, A. Ogata, and T. Tsuchikawa, "Enhanced supercapacitive behaviors of birnessite," *Electrochemistry Communications*, vol. 10, no. 10, pp. 1435–1437, 2008.

[16] L. Athouël, F. Moser, R. Dugas, O. Crosnier, D. Bélanger, and T. Brousse, "Variation of the MnO$_2$ birnessite structure upon charge/discharge in an electrochemical supercapacitor electrode in aqueous Na$_2$SO$_4$ electrolyte," *The Journal of Physical Chemistry C*, vol. 112, no. 18, pp. 7270–7277, 2008.

[17] N. Larabi-Gruet, S. Peulon, A. Lacroix, and A. Chaussé, "Studies of electrodeposition from Mn(II) species of thin layers of birnessite onto transparent semiconductor," *Electrochimica Acta*, vol. 53, no. 24, pp. 7281–7287, 2008.

[18] B. Ma, W. Hou, Y. Han, R. Sun, and Z.-H. Liu, "Exfoliation reaction of birnessite-type manganese oxide by a host-guest electrostatic repulsion in aqueous solution," *Solid State Sciences*, vol. 10, no. 2, pp. 141–147, 2008.

[19] I. Djerdj, D. Arčon, Z. Jagličić, and M. Niederberger, "Nonaqueous synthesis of metal oxide nanoparticles: short review and doped titanium dioxide as case study for the preparation of transition metal-doped oxide nanoparticles," *Journal of Solid State Chemistry*, vol. 181, no. 7, pp. 1571–1581, 2008.

[20] C. Calvert, R. Joesten, K. Ngala, et al., "Synthesis, characterization, and rietveld refinement of tungsten-framework-doped porous manganese oxide (K-OMS-2) material," *Chemistry of Materials*, vol. 20, no. 20, pp. 6382–6388, 2008.

[21] S. Brunauer, P. H. Emmett, and E. Teller, "Adsorption of gases in multimolecular layers," *Journal of the American Chemical Society*, vol. 60, no. 2, pp. 309–319, 1938.

[22] J. I. Morrow and S. Perlman, "A kinetic study of the permanganate-manganous ion reaction to form manganic ion in sulfuric acid media," *Inorganic Chemistry*, vol. 12, no. 10, pp. 2453–2455, 1973.

[23] W. M. Latimer and J. H. Hildebrand, "Reference Book of Inorganic Chemistry," Macmillan, New York, NY, USA, 1951.

[24] M. Villalobos, B. Lanson, A. Manceau, B. Toner, and G. Sposito, "Structural model for the biogenic Mn oxide produced by *Pseudomonas putida*," *American Mineralogist*, vol. 91, no. 4, pp. 489–502, 2006.

[25] O. Giraldo, S. L. Brock, M. Marquez, S. L. Suib, H. Hillhouse, and M. Tsapatsis, "Materials: spontaneous formation of inorganic helices," *Nature*, vol. 405, no. 6782, p. 38, 2000.

[26] X. Wang and Y. Li, "Synthesis and formation mechanism of manganese dioxide nanowires/nanorods," *Chemistry: A European Journal*, vol. 9, no. 1, pp. 300–306, 2003.

[27] S.-H. Yu, H. Cölfen, K. Tauer, and M. Antonietti, "Tectonic arrangement of $BaCO_3$ nanocrystals into helices induced by a racemic block copolymer," *Nature Materials*, vol. 4, no. 1, pp. 51–55, 2005.

[28] A.-C. Gaillot, V. A. Drits, A. Plançon, and B. Lanson, "Structure of synthetic K-Rich birnessites obtained by high-temperature decomposition of $KMnO_4$. 2. Phase and structural heterogeneities," *Chemistry of Materials*, vol. 16, no. 10, pp. 1890–1905, 2004.

[29] J. Y. Shin and M. A. Cheney, "Abiotic transformation of atrazine in aqueous suspension of four synthetic manganese oxides," *Colloids and Surfaces A*, vol. 242, no. 1–3, pp. 85–92, 2004.

[30] S. R. Hall, V. M. Swinerd, F. N. Newby, A. M. Collins, and S. Mann, "Fabrication of porous titania (brookite) microparticles with complex morphology by sol-gel replication of pollen grains," *Chemistry of Materials*, vol. 18, no. 3, pp. 598–600, 2006.

[31] L. A. Estroff and A. D. Hamilton, "At the interface of organic and inorganic chemistry: bioinspired synthesis of composite materials," *Chemistry of Materials*, vol. 13, no. 10, pp. 3227–3235, 2001.

[32] A.-C. Gaillot, B. Lanson, and V. A. Drits, "Structure of birnessite obtained from decomposition of permanganate under soft hydrothermal conditions. 1. Chemical and structural evolution as a function of temperature," *Chemistry of Materials*, vol. 17, no. 11, pp. 2959–2975, 2005.

[33] T. Terada, S. Yamabi, and H. Imai, "Formation process of sheets and helical forms consisting of strontium carbonate fibrous crystals with silicate," *Journal of Crystal Growth*, vol. 253, no. 1–4, pp. 435–444, 2003.